Earth and Planetary Science Letters 296 (2010) 451–458

Contents lists available at ScienceDirect

Earth and Planetary Science Letters

journal homepage: www.elsevier.com/locate/epsl

What can a sessile mollusk tell about neotectonics?

D. Sivan [a], U. Schattner [b,*], C. Morhange [c], E. Boaretto [d,e]

[a] Department of Maritime Civilizations, Charney School of Marine Sciences, and the Leon Recanati Institute for Maritime Studies, University of Haifa, Haifa, 31905, Israel
[b] Dr. Moses Strauss Department of Marine Geosciences, Charney School of Marine Sciences, University of Haifa, 31905, Israel
[c] Aix-Marseille University, CEREGE, B.P. 80 Europôle de l'Arbois, F 13545 Aix-en-Provence, France
[d] Department of Land of Israel Studies and Archaeology, Bar Ilan University, Ramat Gan, 52900, Israel
[e] Radiocarbon Dating and Cosmogenic Laboratory, Kimmel Center for Archaeological Science, Weizmann Institute of Science, 76100 Rehovot, Israel

ARTICLE INFO

Article history:
Received 10 March 2010
Received in revised form 21 May 2010
Accepted 25 May 2010
Available online 20 June 2010

Editor: P. DeMenocal

Keywords:
biological sea level
neotectonics
continental margin
Eastern Mediterranean
Holocene

ABSTRACT

Dendropoma petraeum are fixed vermitids (mollusk) that colonize and construct abrasion platform rims along rocky shorelines. These endemic mollusks are considered good relative sea level indicators in the eastern and the southern Mediterranean, due to their narrow habitat below the sea surface (about ±10 cm). The observed relative sea level values recorded (submerged, uplifted or at present mean sea level) reflect a superposition of eustatic, isostatic, tectonic and possibly local sedimentary instabilities. The present study examines fossil *Dendropoma* samples gathered along the Levant coast, from northern Israel to eastern Turkey. Conventional radiocarbon dates (from Turkey, Syria and partly in Lebanon) and ^{14}C Accelerator Mass Spectrometer (AMS) from Lebanon and Israel yields *Dendropoma* ages ranging through Late Holocene. A numerical model is used for calculating the change in sea level through the Holocene as a function of glacio-hydrology and isostasy of the eastern Mediterranean. Space–time dependent subtractions of the model values are used to eliminate the eustatic component of the relative sea level, in order to obtain the tectonic component. Results show a general northward increase in tectonic uplift of the Levantine coast with different rates in different tectonic segments. This differential uplift corresponds well to the major tectonic segments comprising the Levantine continental margin since the Pleistocene, from the Carmel fault to the East Anatolian fault. Hence, these segments were still active during the last thousands years and even during the last hundreds years. The general trend of northward increase in vertical displacement is predominantly dictated by the convergence between the Sinai and Arabian plates with Anatolia and Eurasia, across the Cyprus arc and Zagros belt; and the secondarily dictated by the northward increase in convergence component across the sinistral Dead Sea Fault plate boundary.

1. Introduction

1.1. Structural and geological setting

The eastern Mediterranean is a tectonically active region dominated by interaction between the Anatolian, African, Arabian and Sinai plates (Fig. 1). Relative motions between these crustal terrains takes place in subduction, continental collision and transform faults, surrounding the Levantine basin (e.g., Salamon et al., 2003; Faccenna et al., 2006; Reilinger et al., 2006; Schattner, 2010). The Levant continental margin is a remnant of the Late Paleozoic–Early Mesozoic continental breakup phases that formed the eastern Mediterranean basin (Garfunkel, 1998). Since the Neogene the northern part of the margin, north of the Carmel structure, is being reactivated due to relative motion between Sinai and Arabian plates along a nearby transform plate boundary — the Dead Sea fault (DSF) (Schattner et al., 2006; Elias et al., 2007; Carton et al., 2009). At present, both Arabian plate and Sinai sub plate are moving northward towards Eurasian plate yet in different rates. The resulting relative slip rate across the Dead Sea fault is 4–5 mm/y (Gomez et al., 2007).

Throughout the quaternary one of the main factors that dictates topographic modifications in the land region extending between the DSF and the Levantine coast is the contractional strike slip motion along the northern DSF (Gomez et al., 2007). This region is faulted, folded, uplifted and divided into structural segments which differ in the amount of vertical uplift by branches of the DSF (Schattner et al., 2006). Most notable are the Carmel and Roum faults, located in northern Israel and southern Lebanon (respectively) (Fig. 1).

Structural segmentation of the northern Levant margin has been demonstrated in multiple studies (Darkal et al., 1990; Butler et al., 1998; Daëron et al., 2001,2005; Ben-Avraham et al., 2006; Schattner et al., 2006; Elias et al., 2007; Schattner and Ben-Avraham, 2007; Carton et al., 2009). According to these studies the margin is divided into four main segments (Fig. 1): the *Galilee–Lebanon* in the south — bounded by the Carmel and Roum faults (south and north); further north lays the *Lebanon Mountains* segment, which consists of the

* Corresponding author.
E-mail address: schattner@sci.haifa.ac.il (U. Schattner).

0012-821X/$ – see front matter © 2010 Elsevier B.V. All rights reserved.
doi:10.1016/j.epsl.2010.05.032

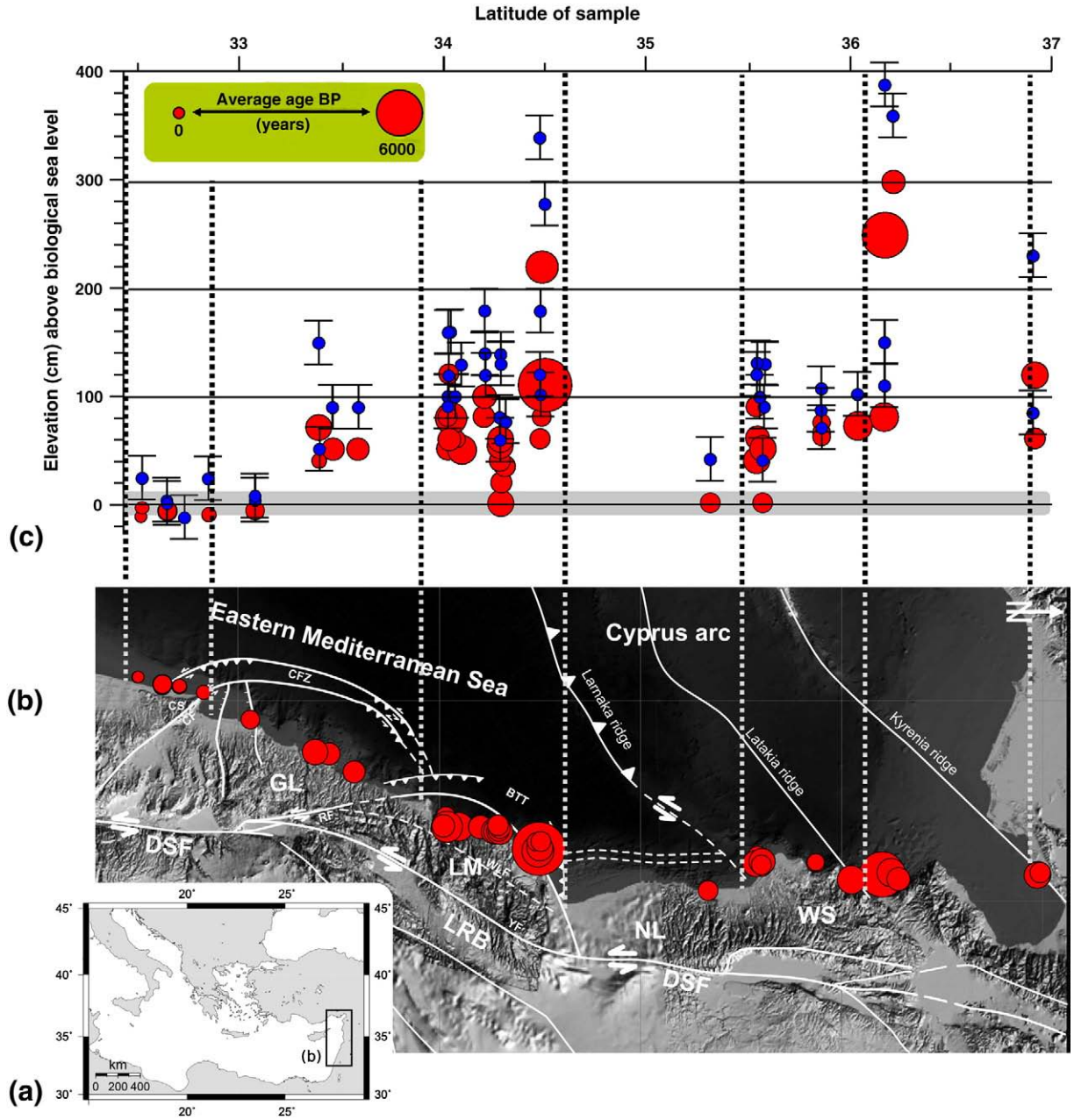

Fig. 1. (a) Location map of the Mediterranean (created using GMT) showing the Levant continental margin. (b) *Dendropoma petraeum* sampling sites are marked (red circles) on the regional DTM (courtesy — J.K. Hall). Circle size denotes the age of the sample in calibrated years before present. White lines denote major plate boundaries and tectonic faults mentioned in the text. The four segments appear as GL = Galilee–Lebanon, LM = Lebanon Mountains, NL = Northern Lebanon, WS = Western Syria. Faults are marked after Westaway (2004) and Schattner et al. (2006). Abbreviations: CS = Carmel structure, CF = Carmel fault, CFZ = Carmel fault zone, RF = Roum fault, WLF, Western Lebanon flexure, LRB = Lebanese restraining bend, DSF = Dead Sea fault. (c) Elevation of K–D contacts above biological sea level plotted against latitude of sampling sites. A gray bar of ± 10 cm marks the error of measurement around the present day sea level. Measured values are marked (red) denoting the sample age in calibrated years before present. Time weighted tectonic displacement calculations are marked (blue) with vertical error bars of ± 20 cm.

Western Lebanon Flexure (Walley, 1998) of the highly elevated part of the Lebanese restraining bend. This segment is bounded to the west by the marine "Beirut–Tripoli thrust" (after Daëron et al., 2001); north of this thrust the *northern Lebanon* segment shows a low laying topography juxtaposed from the south to the Cyprus arc convergent plate boundary. The fourth segment of *western Syria* consists a part of the triple junction between the DSF, East Anatolian fault and the Cyprus arc. Two main ridges of the arc deform the coasts of this segment — Latakia and Larnaka ridges (e.g., Kempler, 1998; Robertson, 1998). Interpretation of these four structural segments was carried out in studies which focused on the Levantine tectonic development during the Plio-Pleistocene.

Several studies also illustrate younger (Late Holocene) vertical displacements in local sites along the coasts of the northern Levant, based on biological and archaeological sea level indicators (Pirazzoli et al., 1991; Sanlaville et al., 1997; Morhange et al., 2006). In these studies sea level changes are interpreted as an indicator for vertical tectonic displacement of the coastline. However, the linkage between sea level change and vertical displacements is not straightforward and needs also a vital ingredient — glacio-hydro-isostatic effect. Hence we adopt Lambeck and Purcell's (2005) numerical model predicting glacio-hydro-isostatic effect on relative sea level across the Mediterranean basin since Last Glacial Maximum. In five contour maps (calculated by Prof. K. Lambeck) we show sea level difference from its

present day elevation at 1000–5000 years BP (Fig. 2). Moreover, to date there is no coherent picture for the neotectonic development of the northern Levant coastline during the Holocene. Here we integrate previous results, add new measurements from the Israeli coasts and use glacio-hydro-isostatic predictions to isolate the different Late Holocene vertical tectonic factor along the above mentioned segments.

1.2. Holocene archaeological sea level indicators along the Levant margin

The Holocene sea level curve of Israel is the most complete and continues curve in the eastern Mediterranean. It is based mainly on a wealth of land and underwater archaeological indicators compared with numerical predictions (Sivan et al., 2001, 2004; Porat et al., 2008). The indicative archaeological remains include coastal man-made cuttings (Galili and Sharvit, 1998; Sivan and Galili, 1999), coastal water wells (Nir and Eldar, 1987; Nir, 1997; Sivan et al., 2004) and man-made structures, such as flushing drainage, sewage channels and quays (used as sea level indicators during their functioning period). Vertical accuracy of these measurements normally ranges between ±2 m for human living floors (Sivan et al., 2001), to about 10–15 cm for coastal water wells (Sivan et al., 2004), ±0.20 m in Roman coastal fish tanks (piscinae) as mentioned in Lambeck et al. (2004a,b). However remains from the Late Holocene and mainly for the last two millennia provide a much smaller error, in the range of few cm. Comparison of the archaeological field data with glacio-hydro-isostatic model predictions indicates vertical tectonic stability of the western northern coast of Israel during the Holocene (Sivan et al., 2001, 2004). Independent geological and archaeological data support the vertical tectonic stability of the coast (Galili and Sharvit, 1998; Sivan and Galili, 1999; Sneh, 2000; Galili et al., 2007). Negligible isostatic crustal movements during the Holocene (Lambeck and Purcell, 2005) makes the Israeli coasts a relative stable reference point for the entire Levantine. However it is not clear whether other locations along the Levantine coast are similarly stable.

2. Sampling and dating the *Dendropoma petraeum* rims

Here we use the *Dendropoma petraeum* bio-indicator to study sea level changes along the Levantine coast. These fixed mollusks, endemic to the eastern, central, and southern Mediterranean region, construct a reef-like structure of variable morphologies at the rims of abrasion platforms (Lipkin and Safriel, 1971; Barash and Zenziper, 1985; Laborel and Laborel-Deguen, 1994; Antonioli et al., 1999). Their narrow habitat is constricted to the upper part of the subtidal zone. Therefore, their upper limit coincides with the "biological sea level" (Laborel and Laborel-Deguen, 1994; Antonioli et al., 1999; Morhange et al., 2006). Hence, the vertical accuracy achieved ranges between ± 10 and 20 cm (Laborel and Laborel-Deguen, 1994; Antonioli et al., 1999; Morhange and Pirazzoli, 2005; Morhange et al., 2006). The lower part of the *Dendropoma* colony, however, marks the biological sea level during the time when the first *Dendropoma* settled on their calcareous sandstone substrate (locally named *Kurkar*). The contact

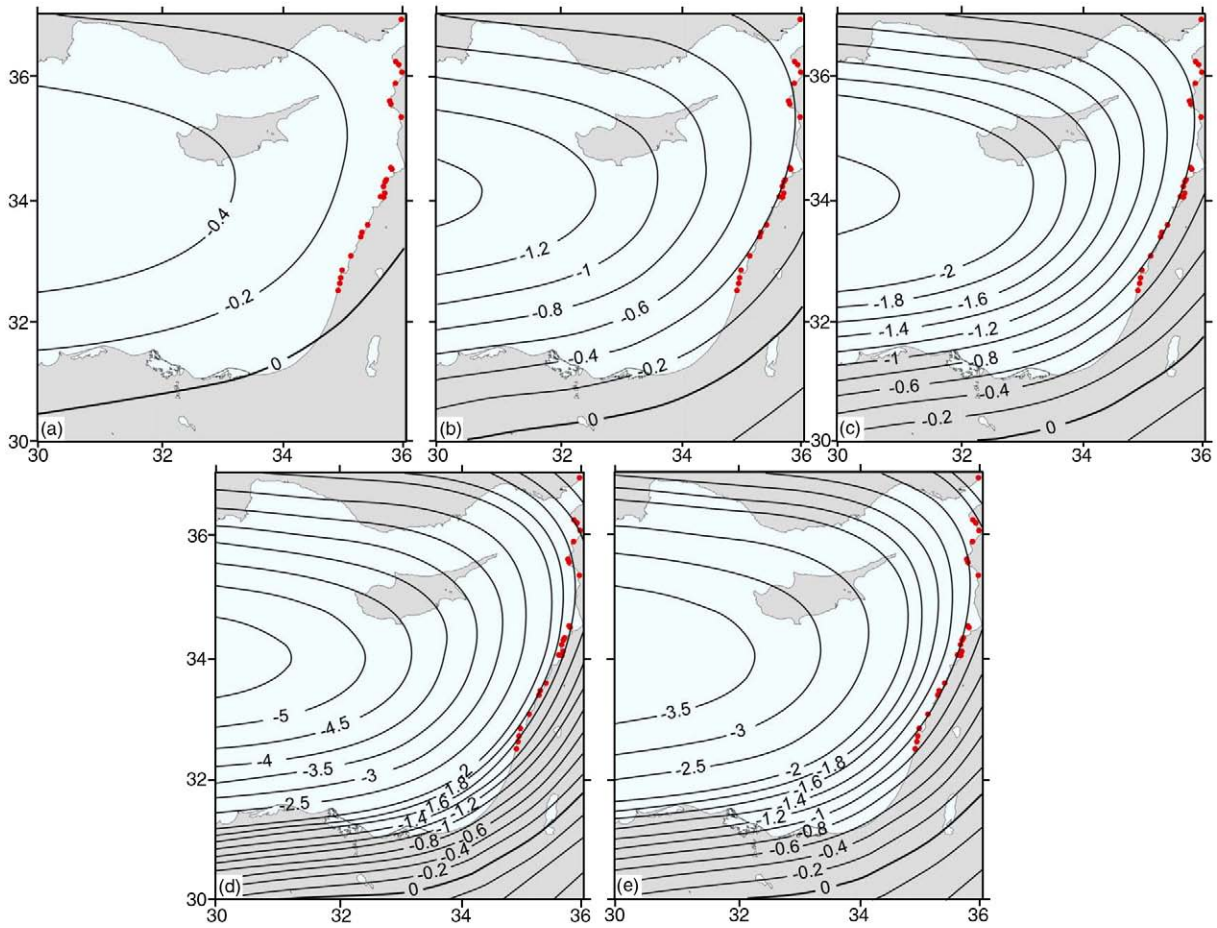

Fig. 2. Predicted sea-levels for (a) 1000 years BP, (b) 2000 years BP, (c) 3000 years BP, (d) 4000 years BP, (e) 5000 years BP, based on Lambeck and Purcell (2005). Values are given in meters relative to the present day mean sea level. These predicted values reflect the ice-volume equivalent sea level contribution, the glacio-isostatic and the hydro-isostatic contribution. Red dots mark the location of the *Dendropoma* sampling sites along the Levant coast.

between the Kurkar substrate and the *Dendropoma* colony is termed here the *K–D* contact (Fig. 3).

2.1. Sampling

Forty cores of *Dendropoma* bio-structures were extracted from edges of abrasion platforms along the coasts of northern Israel (Fig. 3) (Shmueli, 2006). These cores were drilled from the live *Dendropoma* reef (present day biological sea level) vertically down to the K–D contact. Nine of the cores were used for this study (Table 1). Drillings were carried out using a pneumatic drill with a 5 cm cup, powered by compressed air supplied from SCUBA through pressure reducing regulators. In the lab the mineralogy of the K–D contact was analyzed using a Scanning Electron Microscope in the University of Aix-Marseille, France. No diagenetic alterations were found to contaminate the K–D contact, with regards to eligibility for dating.

2.2. Dating

The first *Dendropoma* unit overlying the K–D contact indicates a phase of temporal stabilization of the sea level. This contact was Accelerator Mass Spectrometry (AMS) dated by ^{14}C radiocarbon methods in the nine *Dendropoma* cores from northern coast of Israel. Six of the cores were dated in the Radiocarbon Laboratory of Claude-Bernard University in Lyon, and three in the ETH Institute in Switzerland. Results are shown in Table 1 as calendar years. One of the cores yielded a recent age and hence is omitted from this work.

The Lebanon samples were AMS dated in Lyon, Poznan and Groningen laboratories (Morhange et al., 2006). Those from Syria were dated also in the Radiocarbon Laboratory of Claude-Bernard University in Lyon, by conventional (β counting) method. Those of Turkey were also dated by conventional method, in Paris VI University (Pirazzoli et al., 1991). All ages were corrected for marine reservoir age according to Boaretto et al. (2010), calibrated and are presented as calendar years (Table 1).

A total of 54 samples are integrated and re-evaluated here, all based on the same *Dendropoma* bio-marker: 8 of the samples are from northern Israel (see above), 29 samples from Lebanon, 10 from Syria and 7 from Turkey (Fig. 1; Pirazzoli et al., 1991; Sanlaville et al., 1997; Morhange et al., 2006). These samples establish a state of the art database of abrasion platforms containing *Dendropoma* rims for the easternmost Mediterranean coast (Table 1).

3. Results

3.1. Field data — elevations and dating of the Dendropoma rims

Elevations of K–D contacts vary considerably along the Levantine coast (Figs. 1 and 3). In northern Israel contacts are found in the range of 10–20 cm below the present day biological sea level. Ages of these samples suggest low rates of relative sea level rise during the last millennia, in accordance with Sivan et al. (2004). Further north, however, elevation of K–D contacts range between present day biological sea level and +120 cm — in Lebanon and Syria. These samples range between ~6000 and 6500 years BP. In Turkey sampled K–D contacts were found at +70 cm to +300 cm above the present day biological sea level, with ages ranging between 1500 and 6000 years BP. These wide ranges in K–D contact elevations illustrate

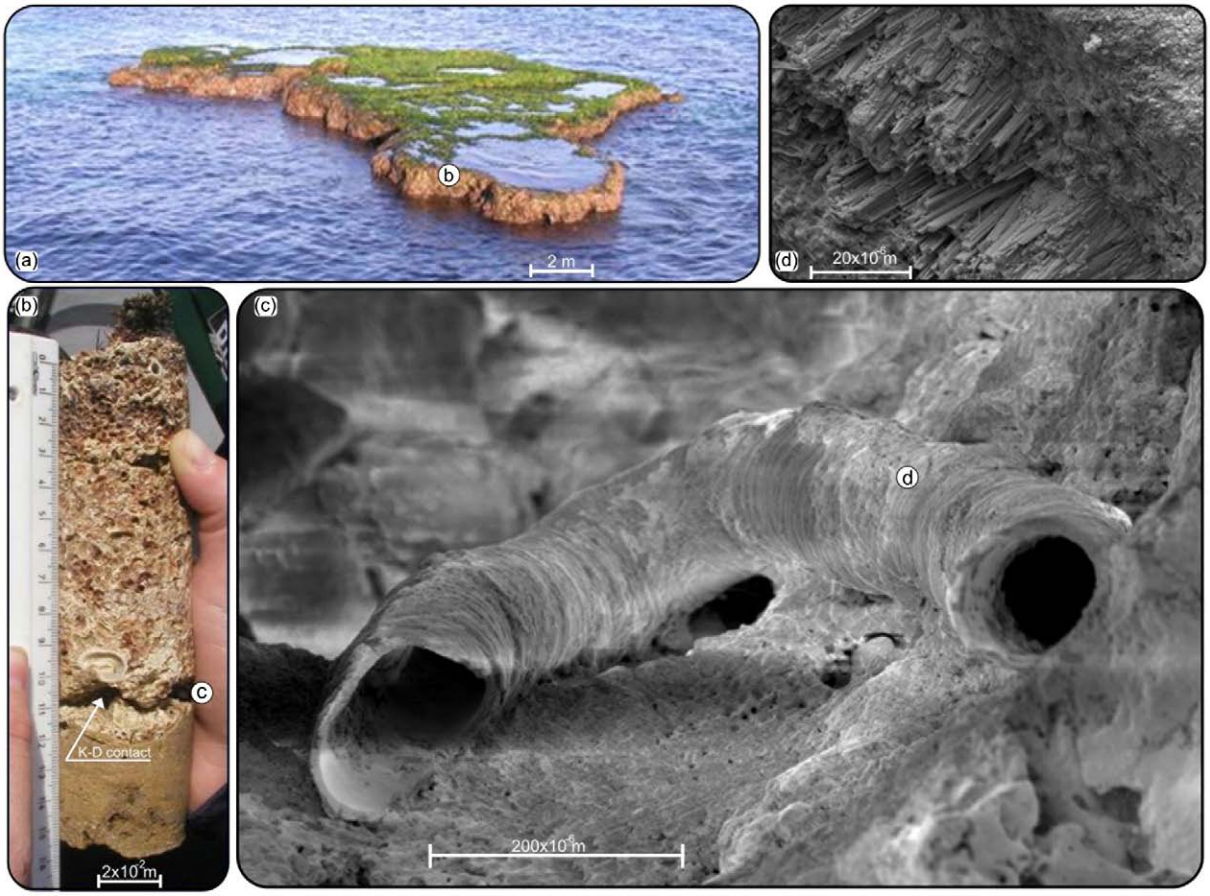

Fig. 3. Four scales of a typical *Dendropoma* sampling site, each denoting the location of the next higher scale: (a) an abrasion platform off northern Israel–Achziv site (Table 1). Sampling was carried out at the rim of the platform. (b) Relative elevation of the K–D contact. (c) A Scanning Electron Microscope image of a *Dendropoma* tube at the K–D contact. (d) Blow-up of the tube showing original aragonite unaltered mineralogy.

Table 1
Data used in this study integrating all *Dendropoma* sampling sites along the Levant coast (Lebanon, Syria and Turkey) with 8 new samples from northern Israel. Tectonic displacement and its rates are calculated values. Table headers' abbreviations: Lat N and Long E — sites location; Elevation (cm) — above biological sea level.

Country	Site	Bio-indicators	Lat N	Long E	Lab. ref.	Elevation (cm)	Elevation uncertainty (cm)	yr^{14}C BP	yr $_{14}$C BP uncertainty $\pm 1\sigma$	Calibrated age relative to $\pm 2\sigma$	Vertical tectonic displacement (cm)	Tectonic displacement rate (mm/y)	Reference
Turkey	Guverdijne Kaya south	*Vermetus* sp.	36.92	35.90	Ly 5623	60	N/A	1890	55	390 AD (95.4%) 650 AD	85	0.60	Sanlaville et al., 1997
			36.92	35.90	Ly 5624	120		5595	85	4260 BC (95.4%) 3830 BC	230	0.38	
	Orontes north	*Dendropoma petraeum*	36.22	35.83	Pa 775	300	20	2595	100	650 BC (95.4%) 0 AD	360	1.58	Pirazzoli et al., 1991
			36.18	35.87	Pa 782	80	10	2040	80	140 AD (95.4%) 550 AD	110	0.69	Sanlaville et al., 1997
			36.18	35.87	Pa 776	80	30	2410	60	300 BC (95.4%) 70 AD	150	0.73	
			36.18	35.87	Pa 779	250	10	4800	80	3340 BC (95.4%) 2900 BC	390	0.71	
			36.05	35.93	Pa 769	72	10	2290	95	200 BC (95.4%) 290 AD	102	0.54	
Syria	Ras el Bassit	*Vermetus* sp.	35.87	35.82	Ly 5622	60	N/A	1335	50	960 AD (95.4%) 1210 AD	70	0.81	Sanlaville et al., 1997
			35.87	35.82	Ly 6266	76		1395	100	780 AD (95.4%) 1230 AD	86	0.91	
			35.87	35.82	Ly 6267	66		1485	50	790 AD (95.4%) 1030 AD	106	1.02	
	Ras Ibn Hani		35.58	35.73	Ly 5625	0		1675	55	610 AD (95.4%) 850 AD	40	0.33	
	Ras el Karm (Ibn Hani)		35.58	35.73	Ly 6283	50		1705	65	560 AD (95.4%) 840 AD	90	0.72	
	Ras Ibn Hani		35.58	35.73	Ly 5621	50		2590	45	410 BC (95.4%) 170 BC	130	0.58	
	Maksar		35.55	35.75	Ly 6273	90		1925	70	300 AD (95.4%) 640 AD	130	0.88	
			35.55	35.75	Ly 6272	60		2360	70	230 BC (95.4%) 150 AD	100	0.52	
			35.55	35.75	Ly 6274	40		2745	65	730 BC (95.4%) 360BC	120	0.48	
	Tell Soukas		35.32	35.93	Ly 6262	1	0.1	1960	50	290 AD (95.4%) 570 AD	41	0.27	
Lebanon	Phare	*Vermetus* sp. and *Corallina*	34.50	35.75	Lyon 1467	110	20	5975	40	4540 BC (95.4%) 4330 BC	280	0.44	Morhange et al., 2006
	Palmier	*Dendropoma petraeum*	34.48	35.77	Ly 10446	80	10	1810	35	500 AD (95.4%) 680 AD	120	0.90	
		Vermetus sp.	34.48	35.77	MC 146	60	N/A	1880	50	410 AD (95.4%) 650 AD	100	0.71	Sanlaville et al., 1997
	Phare	Infra. algae	34.48	35.75	Ly 10447	100	20	2630	35	480 BC (95.4%) 230 BC	180	0.79	Morhange et al., 2006
	Palmier	*Vermetus* sp.	34.48	35.77	MC 145	220	N/A	3490	80	1630 BC (95.4%) 1220 BC	340	1.01	Sanlaville et al., 1997
	Hannouch	*Dendropoma petraeum*	34.30	35.67	Ly 10448	35	15	2195	30	70 AD (95.4%) 250 AD	75	0.42	Morhange et al., 2006
		Vermetus gigas	34.28	35.67	Ly2090	40	15	1930	25	390 AD (95.4%) 560 AD	80	0.54	
	Ras Koubba	*Vermetus* sp.	34.28	35.65	Ly 10445	20	15	2075	35	190 AD (95.4%) 420 AD	60	0.37	
	Selaata	*Dendropoma petraeum*	34.28	35.65	Ly 10444	60	15	2585	35	390 BC (95.4%) 200 BC	140	0.63	
			34.28	35.65	Ly 11580	0	15	2600	30	400 BC (95.4%) 210 BC	80	0.36	
	Koubba		34.28	35.65	Lyon 2091	50	10	2615	25	410 BC (95.4%) 230 BC	130	0.57	
	Selaata		34.28	35.65	Ly 10443	0	15	2750	35	700 BC (1.7%) 680 BC 670 BC (93.7%) 380 BC	80	0.33	
	South Ras Madfoun		34.20	35.63	Lyon 2092	80	10	1995	25	280 AD (95.4%) 480 AD	120	0.77	
	Ras Madfoun		34.20	35.63	Ly 10440	100	10	2340	30	110 BC (95.4%) 90 AD	140	0.72	
			34.20	35.63	Ly 11576	100	10	2410	45	230 BC (95.4%) 50 AD	180	0.89	
			34.20	35.63	Ly 10439	100	10	2485	35	340 BC (95.4%) 80 BC	180	0.85	
	Fidar sud		34.08	35.65	Ly9832	50	10	3020	35	930 BC (95.4%) 760 BC	130	0.47	
	Nahr Ibrahim		34.05	35.63	Ly 11575	60	10	2065	40	190 AD (95.4%) 430 AD	100	0.62	
	North of Bouar	*Balanus* sp.	34.03	35.62	Ly1468	80	10	1160	30	1180 AD (95.4%) 1300 AD	90	1.29	
	Safra	*Dendropoma petraeum*	34.03	35.58	Ly 10386	60	10	1960	35	330 AD (95.4%) 560 AD	100	0.67	
	North of Bouar	Infra. algae	34.03	35.63	Ly 10442	80	10	3195	35	1190 BC (95.4%) 920 BC	160	0.54	
	Tabarja	*Dendropoma petraeum*	34.02	35.62	Ly 10387	80	10	1585	35	700 AD (95.4%) 900 AD	120	1.06	
	South of Tabarja		34.02	35.62	Ly 11574	120	10	1805	30	530 AD (95.4%) 680 AD	160	1.20	
	Tabarja		34.02	35.62	Ly 10437	60	10	1970	35	320 AD (95.4%) 550 AD	100	0.67	
		Infra. algae	34.02	35.62	Ly 10388	50	10	2220	35	30 AD (95.4%) 240 AD	90	0.50	
	Zire–Saida	*Pirenella conica*	33.57	35.37	Lyon 2007	50	20	2210	530	1200 BC (95.4%) 1300 AD	90	0.50	Marriner and Morhange, 2005
	Ras Qantara	*Vermetus triqueter*	33.45	35.28	Lyon 1466	50	20	2230	35	20 AD (95.4%) 230 AD	90	0.50	Morhange et al., 2006
	Hotel Mounes	*Dendropoma petraeum*	33.38	35.27	Ly 11947	40	10	1095	30	1220 AD (95.4%) 1360 AD	50	0.77	
	Ras Abou Zeid	*Vermetus triqueter*	33.38	35.25	Ly 10385	70	20	2525	35	360 BC (95.4%) 140 BC	150	0.69	
Israel	Akziv	*Dendropoma petraeum*	33.06	35.10	LY12274	−3	20	570	45	1650 AD (94.2%) 1890 AD 1940 AD (1.2%) …	7	0.39	Current work
			33.06	35.10	LY12273	−6	20	810	40	1430 AD (95.4%) 1620 AD	4	0.05	
	Atlit		32.71	34.93	ETH29263	−22	20	1195	45	1090 AD (95.4%) 1300 AD	−12	−0.16	
	Shiqmoa		32.83	34.96	ETH29265	−11.5	20	1480	50	790 AD (95.4%) 1030 AD	23.5	0.23	
	Sedot Yam		32.50	34.89	Lyon (OXA)	−12	20	1560	40	720 AD (95.4%) 950 AD	23	0.21	
	Habonim		32.63	34.92	Ly12271	−8.5	20	565	40	1650 AD (95.4%) 1890 AD	1.5	0.03	
	Dor		32.62	34.93	ETH29264	−7	20	560	45	1650 AD (93.3%) 1900 AD 1940 AD (2.1%) …	3	0.05	

the relative change in biological sea level due to local vertical displacement of the sampling sites. Still, the measured elevation values need to be correlated with the time component.

3.2. Extracting the tectonic component

Our working hypothesis is that at a given time biological sea level values (BSL) consist of three components: eustasy (*E*, ice-volume equivalent), glacio-hydro isostasy (GHI) and vertical tectonic (*T*) movements

$$BSL = E + GHI + T$$

BSL values are obtained from field measurements (elevation) and lab analysis (dating). E and GHI predicted values are calculated based on Lambeck and Purcell (2005) for time slices of 1000 years, from 1000 to 6000 BP (Fig. 2). The time slices cover the entire eastern Mediterranean region, however in the subtraction below we used *E* and GHI values at the *Dendropoma* sampling sites. The *T* component may reflect either local or regional (or both) reaction to an applied stress field and thus could predicted by a model. This component is obtained by subtracting the predicted E and GHI values from the observed BSL, for each *Dendropoma* sampling site:

$$T = BSL - E - GHI$$

This calculation is time dependent — taking a BSL elevation value with a known age and subtracting the *E* and GHI value for the corresponding time slice. The quotient represents time weighted finite vertical tectonic (*T*) displacement in centimeters at each *Dendropoma* sampling site. These calculated values are plotted in Fig. 1 together with the measured BSL elevations according to their latitude. Similar to the measured BSL values, the calculated local vertical tectonic displacement varies considerably along the Levantine coast (Table 1): in northern Israel values range between 1.5 and 23.5 cm; Lebanon — between 50 and 340 cm; Syria between 40 and 130 cm; and in Turkey between 85 and 390 cm.

4. Discussion

Elevation and age components of the biological sea level are measurable values. However, they cannot be taken as direct indicators for vertical tectonic displacement at a sampling site because additional, potentially more important components must be taken into consideration — eustasy and glacio-hydro isostasy. This paper isolates the tectonic vertical displacement of sites along the easternmost Mediterranean coast during the Holocene.

4.1. General trend

Tectonic vertical displacement calculated for each of the *Dendropoma* sampling site varies considerably along the eastern Mediterranean coast (Fig. 1). While in northern Israel coastal values are within the range of error (±10 cm) at present day mean sea level, further north values increase up to +390 cm (Orontes north site, Turkey, Table 1). This positive gradient in vertical tectonic displacement could have been explained by elastic bending of the plate. However, studies from the last several decades show that the region is extensively faulted and folded (e.g., Freund and Tarling, 1979; Beydoun, 1981; Ron, 1987; Walley, 1998; Ben-Avraham et al., 2006; Schattner et al., 2006; Elias et al., 2007; Carton et al., 2009). Therefore the gradient suggests a northward increase in brittle failure of the Levantine coast during the Late Holocene.

The tectonic structure and topographic development of the northern Levantine coast during the Pleistocene is dictated by the dynamics of motion along the DSF and its branches (Schattner et al., 2006). Present day, GPS based, plate motion predictions point to convergence across the DSF which intensify northward across the fault axis (Gomez et al., 2007), corresponding to the accentuated topography onland and offshore of Lebanon and Syria. This intensification represents the dominant effect of convergence between the northern flanks of the Sinai and Arabian plates with the eastern Cyprus arc and the Zagros belt (respectively). Our independent results emphasize the northward increase in deformation of the coastline, however the time span of this phenomenon is extended into the Holocene.

4.2. Neotectonics along the Levantine margin

Fig. 1 compares the location of the *Dendropoma* sampling sites with the structural segments of the Levantine margin. The smallest vertical displacement values 1.5 cm (Habonim site, Table 1), calculated for northern Israel, correspond well with the zero displacement reported by Wdowinski et al. (2004) based on GPS measurements. Negligible vertical displacement was also reported based on archaeological evidence: the Galilee coast was stable for the last 3000–4000 years (Sivan and Galili, 1999), while coastal sites in Caesarea indicate stability for the last 2000 years (Sivan et al., 2004). Since northern Israel was shown to be in isostatic equilibrium (Segev et al., 2006) the negligible vertical displacements suggest that it is tectonically stable (vertical displacements) during the last two millennia. Hence any measured change in relative sea level in this region stems conclusively from eustasy.

Further north along the coast of southern Lebanon (*Galilee–Lebanon* structural segment) slightly larger values are calculated for the vertical tectonic displacement, between 50 and 150 cm (sites Zire-Saida, Ras Qantara, Hotel Mounes and Ras Abou Zeid, Table 1; Marriner and Morhange, 2005; Morhange et al., 2006). Along this segment, which is bounded by the Roum fault in the north, the topography becomes progressively more prominent (~1000 m) northwards (Schattner et al., 2006 and references therein). Internal deformations produced by the nearby DSF are manifested by second order southwest trending dextral faults (Ron, 1987; Walley, 1998) which extend to the Levantine coast. Our results show that differential vertical displacement occurs along the coast of the *Galilee–Lebanon* segment during the Holocene.

Much higher displacement values are calculated for the *Lebanon Mountains* segment north and east of the Roum fault. Both this segments and the *Galilee–Lebanon* are located along the Lebanese restraining bend, a right-step of the sinistral DSF along the NNE trending Yammunneh fault (Fig. 1). This slight divergence from the N-striking axis of the DSF induces crustal overlap which is mainly absorbed by north-westward push of the *Lebanon Mountains* segment against the marine Beirut–Tripoli thrust (Schattner et al., 2006 and references therein). The highly elevated topography of this segment (~3000 m) is not in isostatic equilibrium (Segev et al., 2006). It extends from the Lebanon and Anti-Lebanon mountains through the western Lebanon flexure to the coastline, where our results show high displacement values for the Holocene period, ranging between 60 and 340 cm (sites Phare, Palmier, Hannouch, Ras Koubba, Selaata, Ras Madfoun, Fidar sud, Nahr Ibrahim, North of Bouar, Safra, Tabarja, and South of Tabarja, Table 1; Sanlaville et al., 1997; Morhange et al., 2006).

Only one *Dendropoma* site was measured along the coast of the *northern Lebanese* segment (site Tell Soukas, Table 1; Fig. 1; Sanlaville et al., 1997). In this low topography segment the calculated vertical displacement is 41 cm. The site is located closely south to the intersection of the Levantine coast with the Larnaka ridge (part of the Cyprus arc convergence plate margin). North of the Larnaka ridge, however, displacements show higher values, ranging between 40 and 130 cm (sites Ras Ibn Hani, Ras el Karm (Ibn Hani) and Maksar, Table 1; Sanlaville et al., 1997). This jump in displacement values

reflects the active convergence across the easternmost Cyprus arc, where the latter sites are overthrusted.

A similar change in the amount of vertical displacement is observed further north across the Latakia Ridge (part of the Cyprus arc convergence plate margin; Fig. 1). In Ras el Bassit site, south of the ridge, values range between 70 and 106 cm, while north of it vertical displacement extends between 142 and 360 cm — the highest values obtained along the entire margin (sites Orontes north, Table 1; Pirazzoli et al., 1991; Sanlaville et al., 1997). The northernmost sites (sites Guverdijne Kaya south, Table 1; Sanlaville et al., 1997) are also displaced and are located along the Kyrenia–Misis Ridge of the Cyprus arc. Here the values range between 85 and 230 cm, yet no comparable sites were sampled across the ridge.

The detailed comparison above shows a strong agreement between the accepted tectonic segmentation of the Levantine margin and the results of the present work. However, it is important to emphasize that the margin segmentation was previously interpreted as tectonic development during the Plio-Pleistocene time period (Schattner et al., 2006). The results presented here are dated to the Late Holocene period, suggesting that the tectonic segmentation prevails up to recent times, as shown in Elias et al. (2007). Moreover, the clear appearance of vertical tectonic displacement north of the Carmel structure shows that the northern Levantine margin is tectonically active, while the northern Israel coast is tectonically stable for the last two millennia

5. Conclusions

Tectonic vertical displacement values were extracted from 54 sites along the Levantine coast, easternmost Mediterranean. These values are based on time weighted subtraction of glacio-hydro-eustatic predictions of past sea level from field sampling of the *Dendropoma petraeum* bio-indicator (age and elevation) at rims of abrasion platforms. Results show that the northern coast of Israel was tectonically stable during the last two millennia (excluding Haifa bay). Hence, relative sea level fluctuations measured in this part of the Levantine predominantly reflect eustacy and may serve as a reference point for the entire Mediterranean. In this region independent GPS, archaeological and biological indicators for the vertical coastal displacement strongly correlate. This correlation supports the reliability of the *D. petraeum* as a sea level indicator and the conclusion concerning the stability of the Israeli coast.

The general northward increase in vertical displacement along Lebanese, Syrian and Turkish coasts varies in rates. It coincides well with the tectonic segments of the Levantine margin which prevailed during the Quaternary. The results presented here emphasize that these segments continued to deform differently throughout the Holocene. Moreover, the vertical displacements calculated here show that the northern Levantine margin is still tectonically active. This general trend of northward increase in vertical displacement is predominantly dictated by the convergence between the Sinai and Arabian plates with Anatolia and Eurasia, across the Cyprus arc and Zagros belt; and the secondarily dictated by the northward increase in convergence component across the sinistral DSF plate boundary.

Acknowledgements

We would like to thank Sir Maurice and Lady Irene Hatter, from the Recanati Institute for Maritime Studies (RIMS), University of Haifa, for supporting part of the data presented here (from the MA thesis of Mrs. A. Shmueli). We thank Prof. K. Lambeck for providing calculated maps that had a vital role to our study. The authors also thank S. Breitstein and A. Yurman (RIMS diving workshop) for their assistance during the sampling. We thank J. Laborel for his comments and insights. We are grateful for the thorough review by Dr. Mark Siddall and an anonymous reviewer, and for the constructing remarks of EPSL editor Prof. Peter deMenocal.

References

Antonioli, F., Chemello, R., Improt, S., Riggio, S., 1999. *Dendropoma* lower intertidal reef formations and their palaeoclimatological significance, NW Sicily. Mar. Geol. 161, 155–170.

Barash, Al., Zenziper, Z., 1985. Structural and biological adaptations of Vermetidae (Gastropoda). Boll. Malacologico 21, 145–176 Milano.

Ben-Avraham, Z., Schattner, U., Lazar, M., Hall, J.K., Ben-Gai, Y., Neev, D., Reshef, M., 2006. Segmentation of the Levant continental margin, eastern Mediterranean. Tectonics 25, TC5002.

Beydoun, Z., 1981. Some open questions relating to the petroleum prospects of Lebanon. J. Pet. Geol. 3, 303–314.

Boaretto, E., Mienis, H.K., Sivan, D., 2010. Reservoir age based on pre-bomb shells from the intertidal zone along the coast of Israel. Nucl. Instrum. Meth. Phys. Res. B, 268, 966–968.

Butler, R.W.H., Spencer, S., Griffiths, H.M., 1998. The structural response to evolving plate kinematics during transpression: evolution of the Lebanese restraining bend of the Dead Sea Transform. In: Holdsworth, R.E., Strachan, R.A., Dewey, J.F. (Eds.), Continental Transpressional and Transtensional Tectonics: Geological Society, London, Special Publications, 135, pp. 81–106.

Carton, H., Singh, S.C., Tapponier, P., Elias, A., Briais, A., Sursock, A., Jomma, R., King, G.C.P., Daëron, M., Jacques, E., Barrier, L., 2009. Seismic evidence for Neogene and active shortening offshore of Lebanon (Shalimar cruise). J. Geophys. Res. 114, B07407 10.1029/2007JB005391.

Daëron, M., Tapponnier, P., Jacques, E., Elias, A., King, G., Sursock, A., Geze, R., Charbel, A., 2001. Evidence for Holocene Slip and Large Earthquakes on the Yammouneh Fault (Lebanon). Eos. Trans. AGU, Fall Meet. Suppl. Abstract S52D-0666.

Daëron, M., Klinger, Y., Tapponnier, P., Elias, A., Jacques, E., Sursock, A., 2005. Sources of the large A.D. 1202 and 1759 Near East earthquakes. Geology 33, 529–532.

Darkal, A.N., Krauss, M., Ruske, R., 1990. The Levant Fault Zone. Zeitschrift von Geologische Wissenschaft 18, 549–562.

Elias, A., Tapponier, P., Singh, S.C., King, G.C.P., Briais, A., Daëron, M., Carton, S., Sursock, A., Jacques, E., Jomaa, R., Klinger, Y., 2007. Active thrusting offshore Mount Lebanon: Source of the tsunamigenic A.D. 551 Beirut–Tripoli earthquake. Geology 35, 755–758.

Faccenna, C., Bellier, O., Martinod, J., Piromallo, C., Regard, V., 2006. Slab detachment beneath eastern Anatolia: a possible cause for the formation of the North Anatolian fault. Earth Planet. Sci. Lett. 242, 85–97.

Freund, R., Tarling, D.H., 1979. Preliminary Mesozoic paleomagnetic results from Israel and inferences for a microplate structure in the Lebanon. Tectonophysics 60, 189–205.

Galili, E., Sharvit, J., 1998. Ancient coastal installations and the tectonic stability of the Israeli coast in historical times. In: Stewart, I.S., Vita-Finzi, C. (Eds.), Coastal Tectonics: Geological Society, London, Special Publication, Vol. 146, pp. 147–163.

Galili, E., Zviely, D., Ronen, A., Mienis, H.K., 2007. Beach deposits of MIS 5e high sea stand as indicators for tectonic stability of the Carmel coastal plain, Israel. Quatern. Sci. Rev. 26, 2544–2557.

Garfunkel, Z., 1998. Constrains on the origin and history of the eastern Mediterranean basin. Tectonophysics 298, 5–35.

Gomez, F., Karam, G., Khawlie, M., McClusky, S., Vernant, P., Reilinger, R., Jaafar, R., Tabet, C., Khair, K., Barazangi, M., 2007. Global Positioning System measurements of strain accumulation and slip transfer through the restraining bend along the Dead Sea fault system in Lebanon. Geophys. J. Int. 168, 1021–1028.

Kempler, D., 1998. Eratosthenes Seamount: the possible spearhead of incipient continental collision in the eastern Mediterranean. In: Robertson, A.H.F., Emeis, K.-C., Richter, C., Camerlenghi, A. (Eds.), Proceedings of the Ocean Drilling Program, Scientific Results, Vol. 160, pp. 709–721.

Laborel, J., Laborel-Deguen, F., 1994. Biological indicators of relative sea-level variations and of co-seismic displacements in the Mediterranean region. J. Coast. Res. 10, 395–415.

Lambeck, K., Purcell, A., 2005. Sea-level change in the Mediterranean Sea since the LGM: model predictions for tectonically stable areas. Quatern. Sci. Rev. 24, 1969–1988.

Lambeck, K., Antonioli, F., Purcell, A., Silenzi, S., 2004a. Sea level change along the Italian coast for the past 10,000 yrs. Quatern. Sci. Rev. 23, 1567–1598.

Lambeck, K., Anzidei, M., Antonioli, F., Benini, A., Esposito, E., 2004b. Sea level in Roman time in the central Mediterranean and implications for modern sea level rise. Earth Planet. Sci. Lett. 224, 563–575.

Lipkin, Y., Safriel, U., 1971. Intertidal zonation on rocky shores at Mikmoret. J. Ecol. 59, 1–30.

Marriner, N., Morhange, C., 2005. Under the city centre, the ancient harbour. Tyre and Sidon: heritages to preserve. J. Cult. Herit. 6, 183–189.

Morhange, C., Pirazzoli, P.A., 2005. Mid-Holocene emergence of southern Tunisian coasts. Mar. Geol. 220, 205–213.

Morhange, C., Pirazzoli, P.A., Marriner, N., Montaggioni, L.F., Nammour, T., 2006. Late Holocene relative sea-level changes in Lebanon, Eastern Mediterranean. Mar. Geol. 230, 99–114.

Nir, Y., 1997. Middle and late Holocene sea-levels along the Israel Mediterranean coast — evidence from ancient water wells. J. Quatern. Sci. 12, 143–151.

Nir, Y., Eldar, I., 1987. Ancient wells and their geoarchaeological significance in detecting tectonics of the Israel Mediterranean coastline region. Geology 15, 3–6.

Pirazzoli, P.A., Laborel, J., Saliège, J.F., Erol, O., Kayan, I., Person, A., 1991. Holocene raised shorelines on the Hatay coasts (Turkey: paleoecological and tectonic implications). Mar. Geol. 96, 295–311.

Porat, N., Sivan, D., Zviely, D., 2008. Late Holocene embayment and sedimentological infill processes in Haifa Bay, SE Mediterranean. Isr. J. Earth Sci. 57, 21–31.
Reilinger, R., McClusky, S., Vernant, P., Lawrence, S., Ergintav, S., Cakmak, R., Ozener, H., Kadirov, F., Guliev, I., Stepanyan, R., Nadariya, M., Hahubia, G., Mahmoud, S., Sakr, K., ArRajehi, A., Paradissis, D., Al-Aydrus, A., Prilepin, M., Guseva, T., Evren, E., Dmitrotsa, A., Filikov, S.V., Gomez, F., Al-Ghazzi, R., Karam, G., 2006. GPS constraints on continental deformation in the Africa-Arabia-Eurasia continental collision zone and implications for the dynamics of plate interactions. J. Geophys. Res. 111, B05411.
Robertson, A.H.F., 1998. Tectonic significance of the Eratosthenes Seamount: a continental fragment in the process of collision with a subduction zone in the eastern Mediterranean (Ocean Drilling Program Leg 160). Tectonophysics 298, 63–82.
Ron, H., 1987. Deformation along the Yammunneh, the restraining bend of the Dead Sea transform: paleomagnetic data and kinematic implications. Tectonics 6, 653–666.
Salamon, A., Hofstetter, A., Garfunkel, Z., Ron, H., 2003. Seismotectonics of the Sinai subplate — the eastern Mediterranean region. Geophys. J. Int. 155, 149–173.
Sanlaville, P., Dalongeville, R., Bernier, P., Evin, J., 1997. The Syrian coast: a model of Holocene coastal evolution. J. Coast. Res. 13, 385–396.
Schattner, U., 2010. What triggered the early-to-mid Pleistocene tectonic transition across the entire eastern Mediterranean? Earth Planet. Sci. Lett. 289, 539–548.
Schattner, U., Ben-Avraham, Z., 2007. Transform margin of the northern Levant, eastern Mediterranean: from formation to reactivation. Tectonics 26 (TC5020), 1–17.
Schattner, U., Ben-Avraham, Z., Lazar, M., Hübscher, C., 2006. Tectonic isolation of the Levant basin offshore Galilee–Lebanon — effects of the Dead Sea fault plate boundary on the Levant continental margin, eastern Mediterranean. J. Struct. Geol. 28, 2049–2066.
Segev, A., Rybakov, M., Lyakhovsky, V., Hofstetter, A., Tibor, G., Goldshmidt, V., Ben Avraham, Z., 2006. The structure, isostasy and gravity field of the Levant continental margin and the southeast Mediterranean area. Tectonophysics 425, 137–157.
Shmueli, A., 2006. *Dendropoma petraeum*, an indicator of relative sea level change along the northern Israeli coast. MA thesis, Department of Maritime Civilizations, University of Haifa, 34 pp. (in Hebrew, English abstract).
Sivan, D., Galili, E., 1999. Holocene tectonic activity in the coastal and shallow shelf of the western Galilee, Israel, a geological and archaeological study. Isr. J. Earth Sci. 48, 47–61.
Sivan, D., Wdowinski, S., Lambeck, K., Galili, E., Raban, A., 2001. Holocene sea-level changes along the Mediterranean coast of Israel, based on archaeological observations and numerical model. Palaeogeogr. Palaeoclimatol. Palaeoecol. 167, 101–117.
Sivan, D., Lambeck, K., Toueg, R., Raban, A., Porath, Y., Shirman, B., 2004. Ancient coastal wells of Caesarea Maritima, Israel, an indicator for sea level changes during the last 2000 years. Earth Planet. Sci. Lett. 222, 315–330.
Sneh, A., 2000. Faulting in the coastal plain of Israel during the Late Quaternary, re-examined. Isr. J. Earth Sci. 49, 21–29.
Walley, C.D., 1998. Some outstanding issues in the geology of Lebanon and their importance in the tectonic evolution of the Levantine region. Tectonophysics 298, 37–62.
Wdowinski, S., Bock, Y., Baer, G., Prawirodirdjo, L., Bechor, N., Naaman, S., Knafo, R., Forrai, Y., Melzer, Y., 2004. GPS measurements of current crustal movements along the Dead Sea Fault. J. Geophys. Res. 10910.1029/2003JB002640.
Westaway, R., 2004. Kinematic consistency between the Dead Sea Fault Zone and the Neogene and Quaternary left-lateral faulting in SE Turkey. Tectonophysics 391, 203–237.